

#### **OPEN ACCESS**

EDITED BY Fatih Ozogul, Çukurova University, Türkiye

REVIEWED BY
Weibin Wu,
Anhui Agricultural University, China
Veeramani Karuppuchamy,
The Ohio State University, United States

\*CORRESPONDENCE
Enping Zhang

☑ zhangenping@nwafu.edu.cn

RECEIVED 16 July 2025
ACCEPTED 10 September 2025
PUBLISHED 16 October 2025

#### CITATION

Li B, Xu W, Wang W, Mao M, Huang X and Zhang E (2025) Discrepancies in gut microbial communities and serum metabolites of Hu sheep with different backfat thickness. *Front. Microbiol.* 16:1667088. doi: 10.3389/fmicb.2025.1667088

#### COPYRIGHT

© 2025 Li, Xu, Wang, Mao, Huang and Zhang. This is an open-access article distributed under the terms of the Creative Commons Attribution License (CC BY). The use, distribution or reproduction in other forums is permitted, provided the original author(s) and the copyright owner(s) are credited and that the original publication in this journal is cited, in accordance with accepted academic practice. No use, distribution or reproduction is permitted which does not comply with these terms.

# Discrepancies in gut microbial communities and serum metabolites of Hu sheep with different backfat thickness

Bo Li, Wenwen Xu, Wenjia Wang, Mengyuan Mao, Xiaoyu Huang and Enping Zhang\*

College of Animal Science and Technology, Northwest A and F University, Xianyang, China

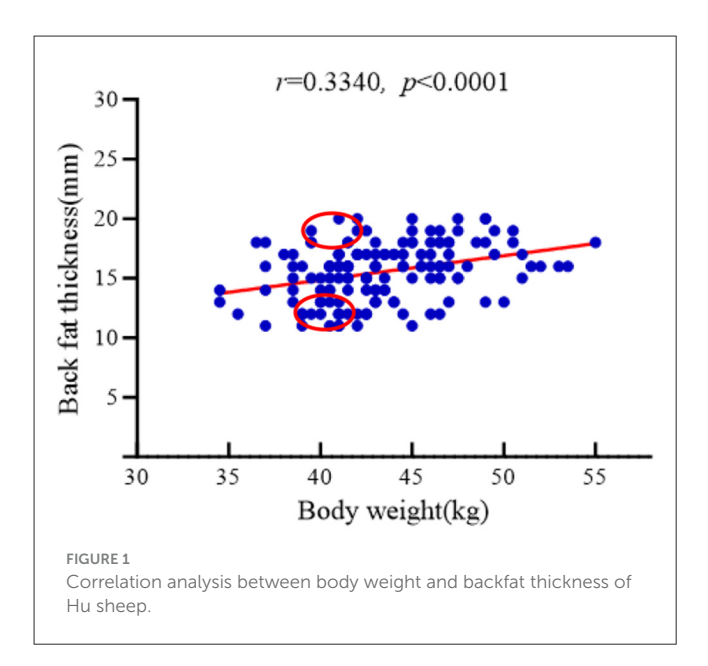
Although market demand for lean meat continues to rise, the regulatory mechanisms governing backfat thickness (BFT) metabolism remain poorly understood. This study employed a multi-omics approach to investigate BFTassociated differences in Hu sheep with distinct fat deposition phenotypes. From 160 genetically similar Hu sheep, we selected 12 individuals with non-significant weight differences (P > 0.05) but extreme divergence in BFT [6 high-BFT (HBF) and 6 low-BFT (LBF) individuals]. Using integrated metagenomics and metabolomics, we systematically compared ileal microbial community structure and serum metabolic profiles between the two groups. HBF sheep showed significantly increased adiposity and altered ileal microbiota composition, characterized by elevated abundances of Carnobacterium, Parabacteroides distasonis, Lactiplantibacillus, and Bifidobacterium. Serum metabolomics glycerophospholipids-1-(9Z-octadecenoyl)-2identified key differential (11Z-eicosenoyl)-glycero-3-phosphate, PE-NMe(15:0/20:3(5Z,8Z,11Z)), PE-NMe<sub>2</sub>(18:1(9Z)/20:0), and PE-NMe<sub>2</sub>(18:1(9Z)/22:1(13Z))-all enriched in glycerophospholipid metabolism pathways. Integrated correlation analysis revealed strong associations between P. distasonis abundance and these phospholipids. These results demonstrate BFT-related adaptive remodeling of the serum metabolome and gut microbiota, identifying P. distasonis as a potential modulator of the host-microbe metabolic axis in ovine adiposity regulation.

KEYWORDS

backfat thickness, metagenomics, serum metabolomics, gut microbiota, sheep

### 1 Introduction

Fat is an essential nutrient in humans and animals, regulating life activities through the absorption of glucose and fatty acids and the secretion of diverse bioactive molecules, including hormones, metabolites, and genetic material (Rosen and Spiegelman, 2014). However, dysregulation of fat secretion can lead to metabolic disorders such as lipid overload, inflammation, and organelle stress, posing risks to health (Julibert et al., 2019; An et al., 2023). Over the long process of domestication, sheep have evolved to deposit substantial fat reserves in subcutaneous tissue and the tail, serving as adaptations to withstand harsh environments and store energy (Cheng et al., 2016). In modern intensive



sheep farming, excessive subcutaneous fat deposition diminishes lean meat yield and impairs animal health, increasing vulnerability to metabolic disorders, inflammation, and reduced disease resistance (Liu et al., 2024). Concurrently, rising consumer health awareness has intensified scrutiny of the link between dietary fat intake and cardiovascular disease risk (Schlesinger et al., 2019; Sacks et al., 2017). Consequently, negative perceptions of high-fat meat products are driving increased market demand for leaner alternatives, presenting new challenges for sheep producers (Diekman and Malcolm, 2009). These converging factors make the regulation of ovine fat deposition a paramount goal for breeders globally.

In livestock production, Backfat Thickness (BFT) serves as a key indicator of ovine fat deposition. Excessive BFT (> 20 mm) diminishes carcass economic value and may impose a greater metabolic burden on the animal, thereby reducing production efficiency (Zhou et al., 2018). Multiple factors contribute to elevated BFT in sheep, encompassing genetics, diet, and management practices (Du et al., 2022; Zhou et al., 2024; Cerdeño et al., 2006). Serum metabolomics offers a novel perspective for investigating fat deposition, enabling further elucidation of fat metabolism molecular mechanisms through metabolite analysis (Bovo et al., 2016). For instance, Yu et al. (2023) utilized serum metabolomics in Qinchuan cattle divergent for BFT, identifying key sphingolipid metabolites implicated in the systemic regulation of backfat thickness. Currently, research on the impact of BFT on ovine meat quality and adipogenesis remains limited, warranting further exploration into the molecular mechanisms underlying ovine lipid deposition.

The intestinal microbiota significantly modulates lipid metabolism, through diverse mechanisms, it influences lipid absorption, synthesis, and breakdown, thereby regulating host adipogenesis (Moszak et al., 2020; Hou et al., 2024). Research indicates that gut microbes enhance lipid absorption and storage by suppressing the expression of the long non-coding RNA Snhg9

(Wang et al., 2023). Moreover, alterations in microbial community composition and function can direct the efficiency and trajectory of lipid metabolism. Supporting this, Kang et al. (2024) investigated correlations between gut microbiota and phenotypic traits in Sunit sheep under varying feeding regimens. Their findings suggest that shifts in lipid metabolism may be partially linked to differences in bacterial populations.

This study is premised on the complex crosstalk between host metabolism and intestinal microbiota composition (Li et al., 2023; Yang et al., 2024). We hypothesize that the compositional profile and metabolic output of the ileal microbiota in Hu sheep modulate host adipogenesis via serum metabolic mediators, consequently influencing backfat thickness (BFT). To test this hypothesis, we employed integrated metagenomic and metabolomic analyses to characterize differences in ileal microbial community structure and associated metabolites in Hu sheep cohorts with shared genetic backgrounds and body weights, but divergent BFT phenotypes. This research aims to elucidate the mechanisms through which microbial community composition and metabolic activity govern host lipid metabolism.

### 2 Materials and methods

### 2.1 Experimental animals and experimental design

A total of 160 unsold Hu sheep ewes (8-month-old) from Xinzhongsheng Sheep Farm (Yulin City, Shaanxi Province) were subjected to body the weight and backfat thickness measurements. Backfat thickness was measured using A-mode ultrasonography (Renco Lean-Meater®, Minneapolis, MN, USA). To examine the relationship between these parameters, body weight data were visualized through scatter plots and analyzed via linear regression. Figure 1 demonstrates a statistically significant positive correlation between backfat thickness and body weight (r = 0.3340, P < 0.001), with both variables adhering to normal distribution patterns. From the cohort of 160 sheep, two experimental groups were established under same body weight (41  $\pm$  0.5 kg) conditions: High Backfat (HBF) group (Backfat thickness =  $19 \pm 0.5$  mm; n = 6) and Low Backfat (LBF) group (Backfat thickness =  $11 \pm 0.5$  mm; n = 6). The dietary information for all participating Hu sheep is presented in Table 1.

### 2.2 Sample collection

On the morning following the completion of the trial period, ileum contents were collected from the 12 Hu sheep in both the HBF and LBF groups. Immediately transfer approximately 10 g of ileal digestate sample into liquid nitrogen for rapid freezing, then store the frozen specimen at  $-80^{\circ}$ C until required for subsequent analytical procedures. Then, in order to balance experimental costs and necessary repetition times, six ileal contents samples were selected from each group for further metabolomic analysis.

TABLE 1 Composition and nutrient levels of basal diets.

Items	Concentrate supplement	Alfalfa hay		
Ingredients %				
Corn	61.54			
Soybean meal	12.32			
Wheat bran	6.15			
DDGS <sup>a</sup>	15.38			
Premix <sup>b</sup>	2.69			
CaHPO <sub>4</sub>	0.92			
NaHCO <sub>3</sub>	0.54			
NaCl	0.31			
Desorbent	0.15			
Total	100.00			
Nutrition levels <sup>c</sup> %				
Dry matter	90.46	90.94		
Crude protein	19.5	7.93		
Ether extract	2.8	0.76		
Neutral detergent fiber	17.84	53.62		
Acid detergent fiber	7.04	31.49		
Phosphorus	1.14	0.27		
calcium	1.91	2.01		
Gross energy, MJ/Kg	16.84	16.70		

<sup>&</sup>lt;sup>a</sup> DDGS stands for Distillers dried grains with soluble.

### 2.3 Serum sampling and analysis

Blood samples were collected with non-anticoagulation vacuum blood vessels before morning feeding after a 12-hr fast the day before slaughter. Serum was harvested following centrifugation at  $3,000 \times g$  for  $10 \, \text{min}$  at  $4 \, ^{\circ}\text{C}$  and subsequently frozen at  $-80 \, ^{\circ}\text{C}$  until analysis. The centrifuge model used in this process is TDL-80–2B, manufactured in Shanghai, China.

The concentrations of serum albumin (ALB), alkaline phosphatase (ALP), alanine aminotransferase (ALT), aspartate aminotransferase (AST), total cholesterol (CHO), high density lipoprotein (HDL), low density lipoprotein (LDL), triglycerides (TG), total protein (TP),  $\gamma$ -glutamylaminotransferase ( $\gamma$ -GT) and superoxide dismutase (SOD) were determined using corresponding commercial kits (Zhongsheng Beikong Biotechnology and Science Inc., Beijing, China) and an automatic biochemical analyzer (BS-420, Shenzhen Mindray Bio-medical Electronics Co., Shenzhen, China).

# 2.4 Metabolic analysis based on liquid chromatography-mass spectrometry (LC-MS)

The sample stored at  $-80^{\circ}$ C was thawed on ice and vortexed for 10 s. A 50  $\mu$ L aliquot of the sample and 300  $\mu$ L of extraction solution (methanol: acetonitrile = 1:4, V/V) containing internal standards were added into a 2 mL microcentrifuge tube. The mixture was vortexed for 3 min and then centrifuged at 12,000 rpm for 10 min at 4°C (The centrifuge model used in this process is TGL-16B, manufactured in Shanghai, China.). A 200 µL aliquot of the supernatant was collected and placed at  $-20^{\circ}$ C for 30 min, followed by centrifugation at 12,000 rpm for 3 min at 4°C. A 180 µL aliquot of the supernatant was transferred for LC-MS analysis. Each sample was analyzed using two LC/MS methods. One aliquot was analyzed under positive ion conditions and eluted from a T3 column (Waters ACQUITY Premier HSS T3 Column,  $1.8\,\mu\text{m}$ ,  $2.1\,\text{mm} \times 100\,\text{mm}$ ) using 0.1% formic acid in water as solvent A and 0.1% formic acid in acetonitrile as solvent B with the following gradient: 5% to 20% in 2 min, increased to 60% in the next 3 min, increased to 99% in 1 min, held for 1.5 min, then returned to 5% mobile phase B within 0.1 min, and held for 2.4 min. The analytical conditions were as follows: column temperature, 40°C; flow rate, 0.4 mL/min; injection volume, 4  $\mu$ L. The second aliquot was analyzed under negative ion conditions using the same elution gradient as the positive mode.

### 2.5 Microbial DNA isolation, metagenomic sequencing, and functional annotation

According to the manufacturer's standard protocol, microbial DNA from the ileal contents was isolated using the E.Z.N.A. (®) Fecal DNA Kit (Omega Bio-tek Inc., Norcross, GA, USA). After genomic DNA extraction, the quality of the isolated DNA was evaluated by 1% agarose gel electrophoresis, and qualified DNA samples were stored at  $-80^{\circ}$ C until subsequent sequencing.

A total of 1 µg of genomic DNA per sample was used as the starting material for library preparation. Sequencing libraries were generated using the NEBNext® Ultra<sup>TM</sup> DNA Library Prep Kit for Illumina (NEB, USA) following the manufacturer's recommendations. Index codes were added to assign sequences to each sample. Briefly, we utilized the Diagenode Bioruptor® UCD-300 TS non-contact focused ultrasound shearing device (Belgium) to fragment DNA samples into an average length of 350 base pairs (bp). DNA fragments were end-polished, A-tailed, and ligated with Illumina adapters. Further PCR amplification was performed to enrich the ligated DNA fragments. PCR products were purified using the AMPure XP system. Libraries were analyzed for size distribution using the Agilent 2,100 Bioanalyzer and quantified using real-time quantitative PCR (qPCR). The clustering of indexcoded samples was performed on a cBot Cluster Generation System according to the manufacturer's instructions. After cluster generation, library preparations were sequenced on an Illumina Nova-Seq platform, and paired-end sequencing was performed to generate reads.

<sup>&</sup>lt;sup>b</sup> The premix provided the following per kg of diet: vitamin A, 3,50,000 IU; biotin, 50 mg; manganese, 1,300 mg; cobalt, 15 mg; vitamin D3: 70,000 IU; niacinamide, 550 mg; zinc, 1,500 mg; calcium, 10%; vitamin E, 1,100 IU; copper, 180 mg; iodine, 20 mg; sodium chloride, 16%; vitamin B6, 1,000 mg; iron, 500 mg; selenium: 8 mg.

<sup>&</sup>lt;sup>c</sup> All nutritional components in the experimental diets were measured according to Chinese National Standards (GB/T). Specific analytical methods included: dry matter (GB/T 6435–2014), crude protein (GB/T 6432–2018), neutral/acid detergent fiber (GB/T 6434–2006), crude fat (GB/T 6433–2006), crude ash (GB/T 6438–2022), calcium (GB/T 6436–2018), and phosphorus (GB/T 6437–2018). Gross energy content was determined using a C6000 bomb calorimeter (Germany).

### 2.6 Microbiome and metabolomics

In the omics data analysis, n=6 indicates six biological replicates were used. For between group differential analysis, Student's t-test was applied when homogeneity of variance was satisfied; otherwise, the Wilcoxon rank-sum test was used, with statistical significance defined at P<0.05. For integrative analysis of microbial metagenomics and metabolomics, we systematically evaluated associations among three key elements through Spearman's rank correlation analysis: 1) the relative abundance of bacterial taxa within the microbial community, 2) previidentified microbial genera, and 3) standardized individual metabolic profiles.

### 2.7 Statistical analysis

Use one-way analysis of unpaired t-test for inter group statistical comparison. Data are expressed as means  $\pm$  standard error of the mean (SEM). Statistical thresholds were designated as follows: P < 0.05 (significant) and  $0.05 \le P < 0.10$  (trend-level). All analyses and visualizations were conducted employing GraphPad Prism 8.0 (San Diego, USA).

### 3 Results

### 3.1 Serum biochemical indices

As summarized in Table 2, the HBF cohort demonstrated significantly higher HDL concentrations vs the LBF group (P < 0.05). Notably, the HBF group exhibited a trend toward elevated LDL and AST levels (0.05 < P < 0.10).

### 3.2 Serum metabolomic characteristics of groups with different BFT

Untargeted serum metabolomic profiling of Hu sheep cohorts was performed using UHPLC-Q-Exactive MS to characterize metabolic disparities between divergent backfat thickness phenotypes (Figure 2a). Multivariate analyses revealed distinct intergroup clustering via PCA and PLS-DA, with model validity confirmed through permutation testing (Figure 2b). The OPLS-DA model demonstrated exceptional robustness (R²Y = 0.997, P = 0.05;  $Q^2 = 0.604$ , P < 0.05), indicating high predictive fidelity (Figure 2c). The identified metabolites were compared with KEGG compound database and HMDB to obtain metabolite classification spectra (Figure 2d). We found that the majority of these metabolites are organic acids and their derivatives in each group, followed by organic heterocyclic compounds and amino acids and their derivatives.

Using Student's t-test (P < 0.05) and variable importance in projection (VIP) values (VIP > 1), a total of 297 differentially expressed metabolites (84 upregulated and 213 downregulated) were identified between the two groups (Figure 3a). The analysis demonstrated significant differences in metabolite levels between the groups (Figure 3b). As shown in Figure 3c,

TABLE 2 Blood nutrients characteristics and antioxidant capacity of the Hu sheep.

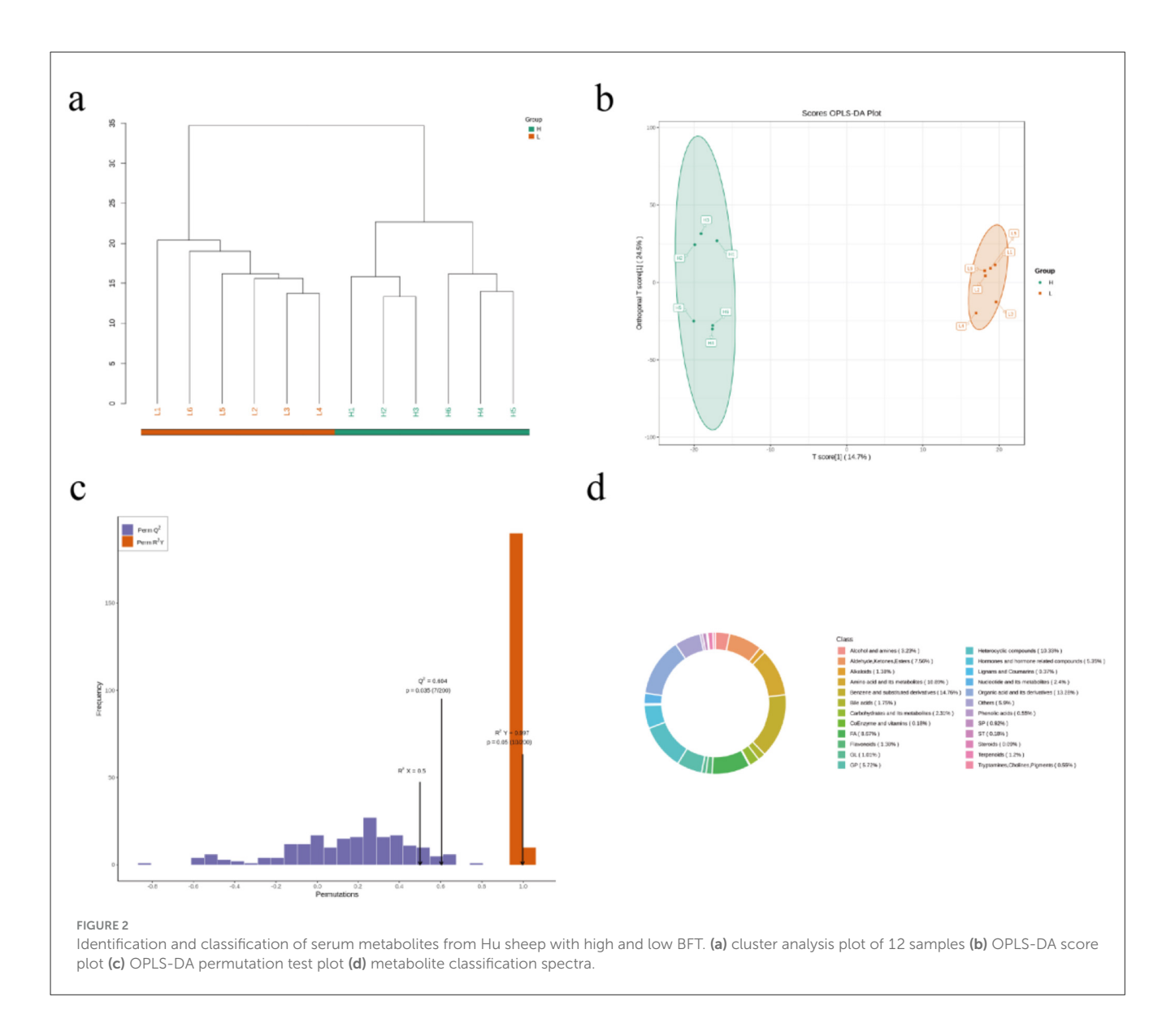
Items	HBF Group	LBF Group	<i>P</i> -value
ALB (g⋅L <sup>-1</sup> )	$28.17 \pm 3.57$	$26.60 \pm 0.96$	0.39
ALP (U·L <sup>-1</sup> )	$224.83 \pm 26.48$	$273.83 \pm 19.95$	0.17
ALT (U·L <sup>-1</sup> )	$18.02 \pm 1.92$	$13.53 \pm 1.9$	0.13
AST (U·L <sup>-1</sup> )	$127.88 \pm 11.89$	$100.55 \pm 6.94$	0.08
CHO (mmol·L <sup>-1</sup> )	$1.71 \pm 1.87$	$1.43 \pm 0.07$	0.18
HDL (mmol⋅L <sup>-1</sup> )	$1.08 \pm 0.08$	$0.85 \pm 0.03$	0.03
LDL (mmol·L <sup>-1</sup> )	$0.77 \pm 0.09$	$0.57 \pm 0.04$	0.09
TG (mmol·L <sup>-1</sup> )	$0.18 \pm 0.02$	$0.19 \pm 0.02$	0.82
TP (g·L <sup>-1</sup> )	$69.27 \pm 3.20$	$66.27 \pm 1.37$	0.41
γ-GT (U·L <sup>-1</sup> )	$52.67 \pm 3.05$	$54.50 \pm 2.06$	0.63
SOD (U⋅mL <sup>-1</sup> )	$135.83 \pm 13.20$	$136.50 \pm 8.53$	0.97

these metabolites were primarily enriched in the following metabolic pathways: fat digestion and absorption, glycerolipid metabolism, glycerophospholipid metabolism, and primary bile acid biosynthesis. Significantly altered metabolites included 1-(9Z-octadecenoyl)-2-(11Z-eicosenoyl)-glycero-3-phosphate, PE-NMe (15:0/20:3[5Z,8Z,11Z]), PE-NMe2 (18:1[9Z]/20:0), PE-NMe2 (18:1[9Z]/22:1[13Z]), and Coenzyme Q8 (Figure 3d). Among these, 1-(9Z-octadecenoyl)-2-(11Z-eicosenoyl)-glycero-3-phosphate, PE-NMe (15:0/20:3[5Z,8Z,11Z]), PE-NMe2 (18:1[9Z]/20:0), and PE-NMe2 (18:1[9Z]/22:1[13Z]) are involved in glycerophospholipid metabolism (Figure 3e).

## 3.3 Prediction of diversity, composition, and function of intestinal bacterial communities

Gut microbiota differences among experimental groups were analyzed using metagenomic sequencing. Functional annotation of sequencing data against the KEGG database revealed functional profiles and taxonomic abundance. No significant differences in alpha diversity were observed between groups (Figure 4a). Principal coordinates analysis (PCoA) demonstrated distinct clustering of microbial community structures (Figure 4b). At the phylum level, Firmicutes, Proteobacteria, Campylobacterota, and Actinobacteriota predominated (Figure 4c). Dominant genera included Staphylococcus, Streptococcus, Enterococcus, and Klebsiella (Figure 4d). Metastats analysis identified significant inter-group differences in microbial composition and function, revealing the top 20 differentially abundant genera (Figure 4e) and top 30 differentially abundant KEGG features (Figure 4f). Notably, the HBF group exhibited significantly higher relative abundances of Enterobacter, Parabacteroides, and Lactiplantibacillus compared to the LBF group (P < 0.05).

Functional profiling of the microbiome was assessed through annotation of genes encoding Carbohydrate-Active Enzymes (CAZymes). Protein sequences derived from non-redundant



gene catalogs were classified into the six primary CAZyme classes. Among these, Glycoside Hydrolases (GHs) and Glycosyl Transferases (GTs) constituted the most abundant classes (Figure 5a). Notably, CAZyme families PL35, CE13, GT24, and GT15 exhibited significant differential abundance between the experimental groups (Figure 5b). KEGG pathway analysis revealed that microbial gene functions were predominantly enriched in pathways associated with lipid metabolism, including the sphingolipid signaling pathway, yeast MAPK signaling pathway, p53 signaling pathway, and arachidonic acid metabolism (Figure 5c).

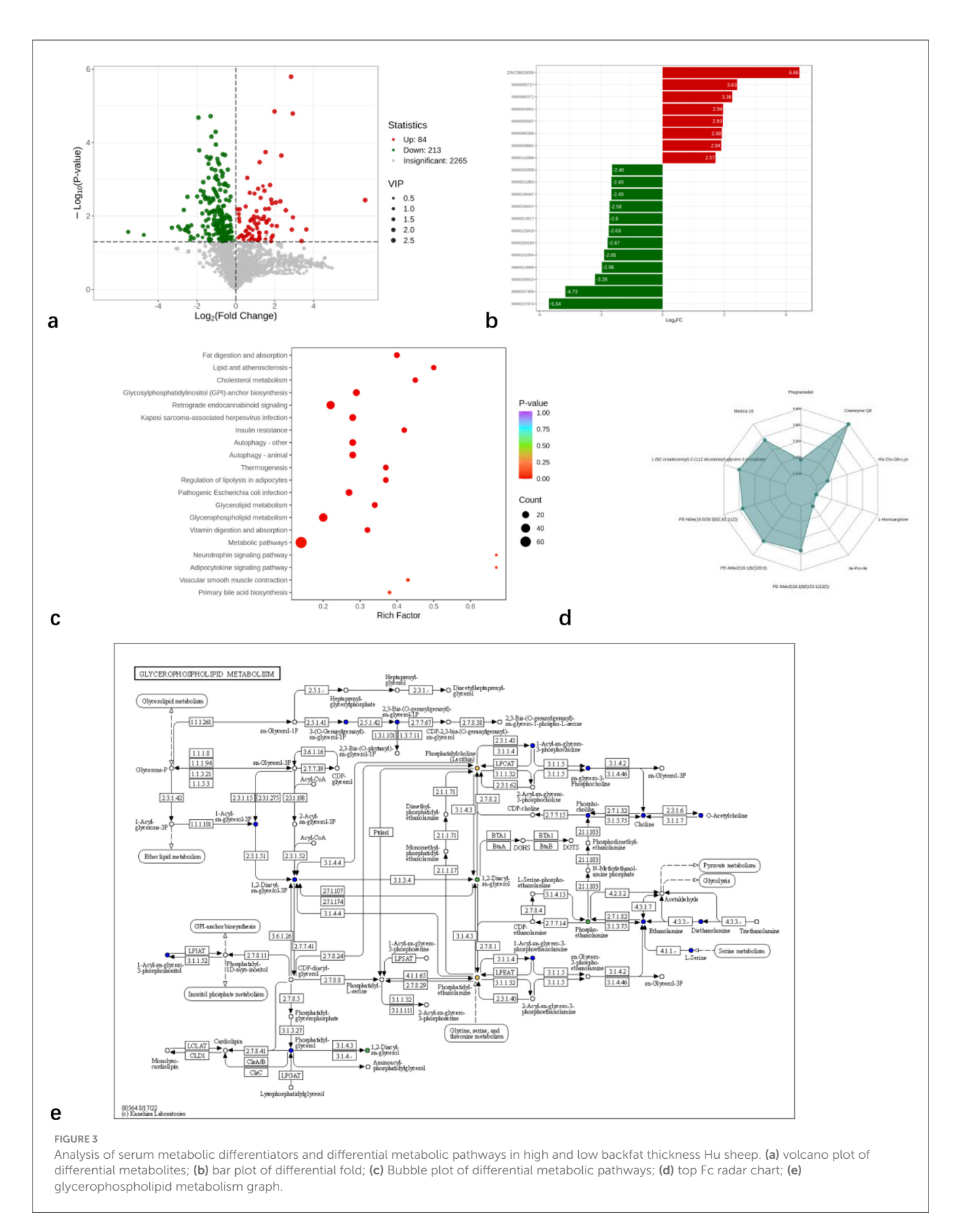
### 3.4 Gut microbiota and metabolome

In order to determine the correlation between serum metabolites and gut microbiota, Spearman's correlation analysis was conducted. According to the association analysis between bacteria and lipid metabolites and fatty acids, intestinal bacteria

may also affect lipid metabolism in the body to some extent. As shown in Figure 6A, *Parabacteroids* are positively correlated with 1-(9Z-octadecenoyl)-2-(11Z-eicosenoyl)-glycero-3-phosphate, PE-NMe (15:0/20:3[5Z,8Z,11Z]), PE-NMe2 (18:1[9Z]/20:0). Building upon the *Parabacteroides* species identified in Figure 6A as significantly correlated with serum metabolites, we performed Pearson correlation analysis between *Parabacteroides* and key phenotypic traits from our prior research (intramuscular fat content - IMF, backfat thickness, subcutaneous adipose tissue mass, GR value, shear force, and C20:3 n-6) (Li et al., 2025). As shown in Figure 6B, *Parabacteroides distasonis* exhibited significant positive correlations with backfat thickness, subcutaneous adipose tissue mass, and GR value, whereas a significant negative correlation was observed with meat tenderness, as measured by shear force.

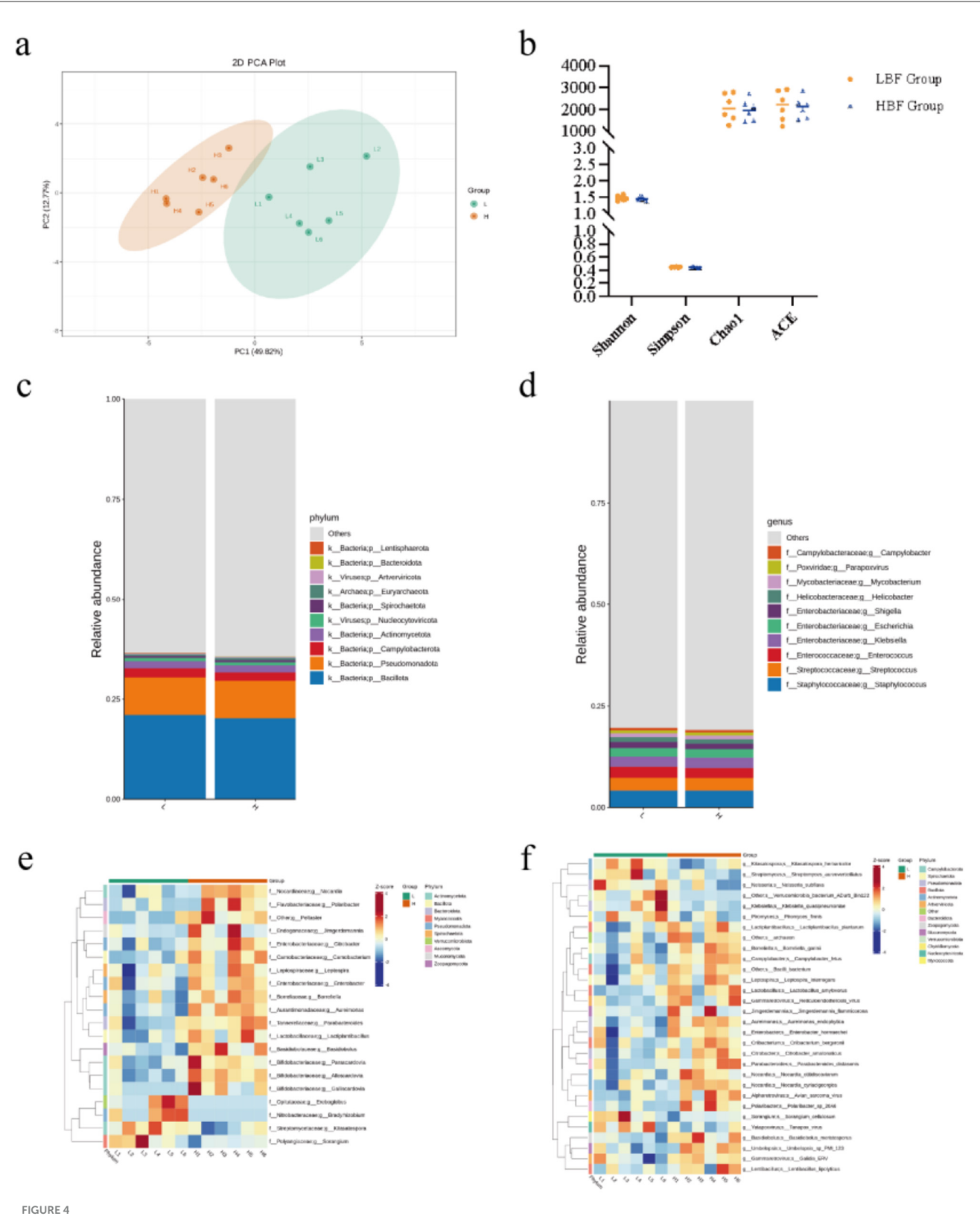
### 4 Discussion

Serum biochemical indicators serve as crucial biomarkers for evaluating an organism's production performance, physiological

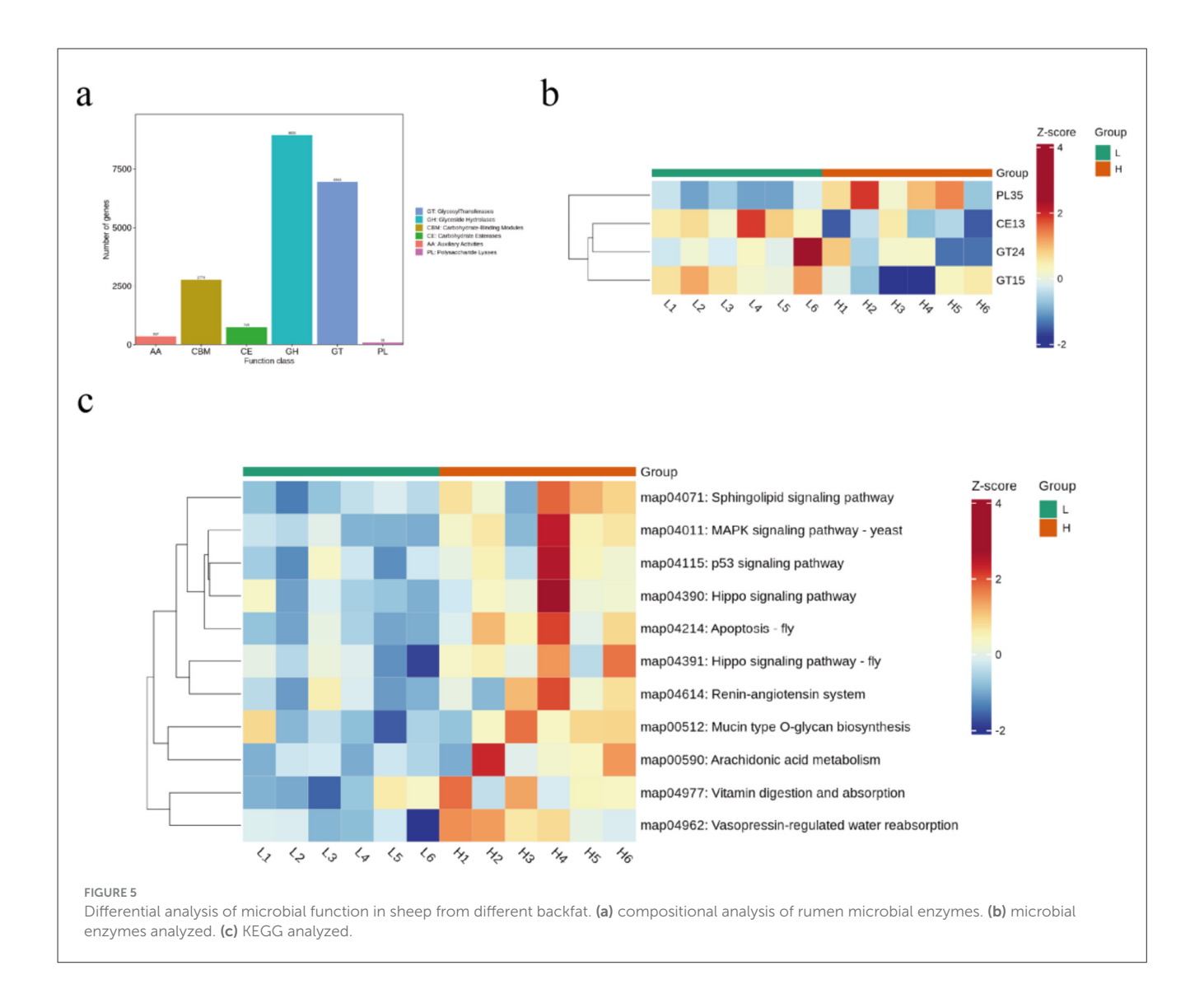


status, and health condition (Jiao et al., 2024). HDL and LDL not only regulate normal lipid metabolism but also exhibit altered levels as key features of metabolic disorders (Durand et al., 1987). AST,

primarily found in tissues such as liver and myocardium, typically elevates in serum following tissue damage or metabolic dysfunction (Mihas et al., 1981). In this study, sheep with HBF group



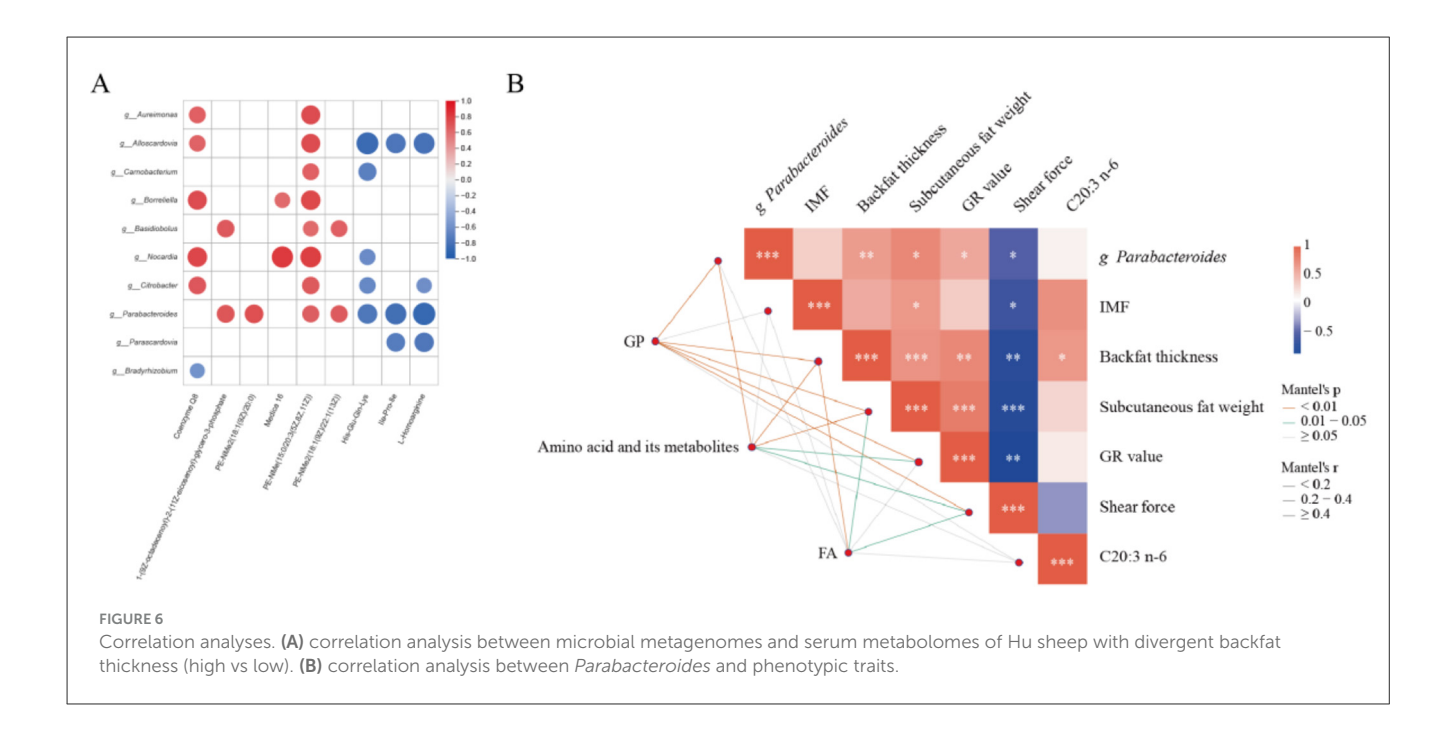
Metagenomic sequencing was used to analyze the composition and functional characteristics of the ileal microbiota of high BFT and low BFT Hu sheep. (a) statistical plot of microbial community diversity and total species. (b) PCoA principal component analysis plot. (c) Kingdom and phylum level community composition stacked bar chart. (d) family and genus level community composition stacked bar chart. (e) heat map of genus level and differential microorganisms. (f) heat map of differential strains at species level.



demonstrated significantly higher HDL levels. This observation may be attributed to HDL's essential role in lipid metabolism—facilitating reverse cholesterol transport from peripheral tissues to the liver for catabolism and excretion, thereby maintaining cholesterol homeostasis (Liang et al., 2020). Concurrently, excessive adipose tissue accumulation may promote cholesterol synthesis and secretion, consequently elevating LDL levels (Aguilar et al., 2014). Furthermore, heightened lipid metabolism in high-backfat sheep could exert physiological stress on hepatic tissues, potentially explaining the observed increase in AST levels (Xie et al., 2022). Grzybowska et al. (2023) found a significant correlation between backfat thickness and blood AST concentration in fatty liver cows. This is similar to the results of this study, suggesting that high backfat thickness may increase the risk of liver health in sheep.

Phosphatidylcholine (PC) and phosphatidylethanolamine (PE) represent the primary and secondary most abundant phospholipids, respectively, with PE serving as a metabolic precursor for PC biosynthesis (Yang et al., 2018). TG and BA concentrations significantly correlate with adiposity and metabolic disorders (Gong et al., 2024; Huang et al., 2025). In the HBF cohort, levels of specific glycerophospholipids

including PE (22:6[4Z,7Z,10Z,13Z,16Z,19Z]/18:1[11Z]), PE-NMe<sub>2</sub> (18:2[9Z,12Z]/24:1[15Z]), and PE-NMe (15:0/20:3[5Z,8Z,11Z]) were markedly higher compared to LBF controls. This phospholipid signature suggests enhanced lipid metabolic flux in HBF sheep, potentially contributing to increased backfat deposition. Branchedchain amino acid abundance further associates with dysregulated lipid homeostasis (Lackey et al., 2013). Dietary lipid catabolism, mediated by pancreatic lipase and other hydrolases, generates absorbable metabolites for energy production and essential fatty acid provision (Omer and Chiodi, 2024). Key metabolic pathways governing these processes include glycerolipid metabolism, which regulates triacylglycerol biosynthesis/catabolism and substrate interconversion (Prentki and Madiraju, 2008); glycerophospholipid metabolism, essential for maintaining membrane phospholipid dynamics critical to cellular integrity (Hermansson et al., 2011); and primary bile acid biosynthesis, facilitating cholesterol conversion and enterohepatic circulation while demonstrating direct implications in lipid disorders when dysregulated (Cai et al., 2022). These metabolic processes are critical determinants of serum lipid profiles, with their dysregulation directly impacting circulating metabolite levels and contributing to systemic.



Gut microbiota composition and activity critically modulate obesity development (Lin et al., 2022). Notably, Carnobacterium spp. and Parabacteroides distasonis demonstrate therapeutic potential against metabolic dysregulation, attenuating weight gain, hyperglycemia, hyperlipidemia, and hepatic steatosis (Qiu et al., 2024; Li et al., 2022). Similarly, probiotic supplementation with Bifidobacterium spp. ameliorates obesity through metabolic reprogramming (Kim et al., 2022), while Lactiplantibacillus plantarum HNU082 enhances lipid catabolism and stabilizes dysbiosis during hyperlipidemia (Shao et al., 2017). Metagenomic analysis identified Carnobacterium, Parabacteroides, Lactiplantibacillus, and Bifidobacterium as the most differentially abundant genera, with P. distasonis exhibiting maximal species-level differentiation. These taxa potentially govern ovine lipid metabolism and backfat deposition.

PL35, a polysaccharide lyase that facilitates oligosaccharide cleavage (Lu et al., 2024), which was significantly elevated in the HBF group, suggesting enhanced oligosaccharide utilization by gut microbiota in this group. Glycosyltransferases (GTs) catalyze the synthesis of glycosidic linkages by transferring sugar residues from donor to acceptor molecules (Lairson et al., 2008). Carbohydrate Esterases (CEs) involve enzymes that catalyze de-O or de-Nacylation to remove ester decorations from carbohydrates (Cantarel et al., 2009). Carbohydrate Esterase family 13 (CE13), the smallest among CE families (Nakamura et al., 2017), along with GT24 and GT15, were significantly elevated in the LBF group. We hypothesize that CE13-mediated deacylation might affect Short-Chain Fatty Acid production, while GT24/GT15 could participate in bile acid glycosylation, modifying their fat emulsification capacity and ultimately impacting host lipid metabolism. For KEGG pathway analysis, microbial gene functions were primarily enriched in lipidogenesis-related pathways including Sphingolipid signaling pathway, MAPK signaling pathway - yeast, p53 signaling pathway, and Arachidonic acid metabolism. Collectively, these findings indicate that alterations in sheep gut microbiota composition lead to functional shifts, with lipid deposition playing a critical role in this process. However, the specific mechanistic pathways involved require further investigation.

Parabacteroides species generate acetic acid and succinate as primary saccharolytic metabolite (Sakamoto and Benno, 2006). Notably, P. distasonis supplementation ameliorates weight gain, hyperglycemia, and hepatic steatosis in metabolic disorder models (Wang et al., 2019). While the succinate/SUCNR1 signaling axis is implicated in obesity pathogenesis (Keiran et al., 2019), its association with serum metabolite profiles remains unexplored. Integrated KEGG analysis of serum metabolomics identified lipid metabolism-associated phospholipids: 1-(9Zoctadecenoyl)-2-(11Z-eicosenoyl)-glycero-3-phosphate, PE-NMe (15:0/20:3[5Z,8Z,11Z]), PE-NMe<sub>2</sub> [18:1(9Z]/20:0), and PE-NMe<sub>2</sub> (18:1[9Z]/22:1[13Z]). Critically, robust covariance was observed between these phospholipids and Parabacteroides abundance. These findings suggest Parabacteroides modulates host lipid homeostasis through serum glycerol-phospholipid remodeling pathways, though precise mechanistic underpinnings warrant further investigation.

### 5 Conclusion

This study preliminarily revealed the dynamic changes in gut microbiota structure and serum metabolites associated with differential backfat thickness in sheep. *Parabacteroides spp.* was identified as discriminant microorganisms distinguishing different backfat thicknesses. Key metabolites involved in glycerophospholipid metabolism included 1-(9Z-octadecenoyl)-2-(11Z-eicosenoyl)-glycero-3-phosphate, PE-NMe (15:0/20:3[5Z,8Z,11Z]), PE-NMe2 (18:1[9Z]/20:0), PE-NMe2 (18:1[9Z]/22:1[13Z]). The findings provide novel insights into the association between serum metabolites and gut microbiota in sheep with varying backfat thickness, while uncovering potential

mechanisms through which microbiota may influence host lipid metabolism via metabolites. This research offers valuable references for understanding lipid metabolism regulation in ruminants. It should be noted that functional validation of *Parabacteroides distasonis* on ovine lipid metabolism has not been performed in the current work. Subsequent studies intend to conduct targeted functional verification experiments for this specific strain.

### Data availability statement

The original contributions presented in the study are publicly available. This data can be found here: PRJCA044305, and publicly available datasets were analyzed in this study. This data can be found here: PRJCA044366.

### **Ethics statement**

The animal studies were approved by the experimental procedure and recommendations for slaughtering Hu sheep in this study have been approved by the Ethics Committee of the Animal Center at Northwest A&F University (IACUC 2024-0920). The studies were conducted in accordance with the local legislation and institutional requirements. Written informed consent was obtained from the owners for the participation of their animals in this study.

### **Author contributions**

BL: Methodology, Software, Writing – original draft. WX: Software, Writing – original draft, Investigation, Supervision. WW: Data curation, Writing – original draft, Visualization. MM: Writing – original draft, Validation, Visualization. XH: Funding acquisition, Writing – review & editing. EZ: Writing – original draft, Visualization.

### References

Aguilar, D., deOgburn, R. C., Volek, S., and Fernandez, M. L. (2014). Cholesterol-induced inflammation and macrophage accumulation in adipose tissue is reduced by a low carbohydrate diet in guinea pigs. *Nutr. Res. Pract.* 8, 625–631. doi: 10.4162/nrp.2014.8.6.625

An, S. M., Cho, S. H., and Yoon, J. C. (2023). Adipose tissue and metabolic health. *Diabetes Metab J.* 47, 595–611. doi: 10.4093/dmj.2023.0011

Bovo, S., Mazzoni, G., Galimberti, G., Calò, D. G., Fanelli, F., Mezzullo, M., et al. (2016). Metabolomics evidences plasma and serum biomarkers differentiating two heavy pig breeds. *Animal* 10, 1741–1748. doi: 10.1017/S1751731116000483

Cai, J., Rimal, B., Jiang, C., Chiang, J. Y. L., and Patterson, A. D. (2022). Bile acid metabolism and signaling, the microbiota, and metabolic disease. *Pharm. Ther* 237:108238. doi: 10.1016/j.pharmthera.2022.108238

Cantarel, B. L., Coutinho, P. M., Rancurel, C., Bernard, T., Lombard, V., and Henrissat, B. (2009). The Carbohydrate-Active EnZymes database (CAZy): an expert resource for Glycogenomics. *Nucleic Acids Res.* 37, D233–D238. doi:10.1093/nar/gkn663

Cerdeño, A., Vieira, C., Serrano, E., Lavín, P., and Mantecón, A. R. (2006). Effects of feeding strategy during a short finishing period on performance, carcass and meat quality in previously-grazed young bulls. *Meat Sci.* 72, 719–726. doi: 10.1016/j.meatsci.2005.10.002

### **Funding**

The author(s) declare that financial support was received for the research and/or publication of this article. This work was supported by the Shaanxi Provincial Key Core Technology Research Project in Agriculture -Genetic Improvement and Integrated Application of Quality and Efficiency Enhancement Technologies for Beef and Mutton Cattle and Sheep (2024NYGG005) and the construction of Yulin Husbandry Industry Research Institute.

### Conflict of interest

The authors declare that the research was conducted in the absence of any commercial or financial relationships that could be construed as a potential conflict of interest.

### Generative AI statement

The author(s) declare that no Gen AI was used in the creation of this manuscript.

Any alternative text (alt text) provided alongside figures in this article has been generated by Frontiers with the support of artificial intelligence and reasonable efforts have been made to ensure accuracy, including review by the authors wherever possible. If you identify any issues, please contact us.

### Publisher's note

All claims expressed in this article are solely those of the authors and do not necessarily represent those of their affiliated organizations, or those of the publisher, the editors and the reviewers. Any product that may be evaluated in this article, or claim that may be made by its manufacturer, is not guaranteed or endorsed by the publisher.

Cheng, X., Zhao, S. G., Yue, Y., Liu, Z., Li, H. W., and Wu, J. P. (2016). Comparative analysis of the liver tissue transcriptomes of Mongolian and Lanzhou fat-tailed sheep. *Genet. Mol. Res.* 15. doi: 10.4238/gmr.15028572

Diekman, C., and Malcolm, K. (2009). Consumer perception and insights on fats and fatty acids: knowledge on the quality of diet fat. *Ann. Nutr. Metab.* 54, 25–32. doi: 10.1159/000220824

Du, L., Li, K., Chang, T., An, B., Liang, M., Deng, T., et al. (2022). Integrating genomics and transcriptomics to identify candidate genes for subcutaneous fat deposition in beef cattle. *Genomics*. 114:110406. doi: 10.1016/j.ygeno.2022.110406

Durand, P., Cathiard, A. M., Naaman, E., Brieu, V., and Saez, J. M. (1987). The influence of plasma lipoproteins on steroidogenesis of cultured ovine fetal and neonatal adrenal cells. *J. Steroid Biochem.* 26, 425–431. doi: 10.1016/0022-4731(87) 90051-3

Gong, J., Zhang, Q., Hu, R., Yang, X., Fang, C., Yao, L., et al. (2024). Effects of *Prevotella copri* on insulin, gut microbiota and bile acids. *Gut Microbes*. 16:2340487. doi: 10.1080/19490976.2024.2340487

Grzybowska, D., Sobiech, P., and Tobolski, D. (2023). Ultrasonographic image of fatty infiltration of the liver correlates with selected biochemical parameters and back fat thickness of periparturient Holstein-Friesian cows. *Pol. J. Vet. Sci.* 26, 723–732. doi: 10.24425/pjys.2023.148292

- Hermansson, M., Hokynar, K., and Somerharju, P. (2011). Mechanisms of glycerophospholipid homeostasis in mammalian cells. *Prog. Lipid Res.* 50, 240–257. doi: 10.1016/j.plipres.2011.02.004
- Hou, M., Ye, M., Ma, X., Sun, Y., Yao, G., Liu, L., et al. (2024). Colon microbiota and metabolite potential impact on tail fat deposition of Altay sheep. *Microbiol. Spectr.* 12:e0310323. doi: 10.1128/spectrum.03103-23
- Huang, Y., Sulek, K., Stinson, S. E., Holm, L. A., Kim, M., Trost, K., et al. (2025). Lipid profiling identifies modifiable signatures of cardiometabolic risk in children and adolescents with obesity. *Nat. Med.* 31, 294–305. doi: 10.1038/s41591-024-03279-x
- Jiao, N., Feng, W., Ma, C., Li, H., Zhang, J., Zheng, J., et al. (2024). Effects of dietary protein levels on digestion, metabolism, serum biochemical indexes, and Rumen Microflora of Lanzhou fat-tailed sheep. *Animals* 15:25. doi: 10.3390/ani15010025
- Julibert, A., Bibiloni, M. D. M., and Tur, J. A. (2019). Dietary fat intake and metabolic syndrome in adults: a systematic review. *Nutr. Metab Cardiovasc. Dis.* 29, 887–905. doi: 10.1016/j.numecd.2019.05.055
- Kang, L., Wang, W., Yang, L., Liu, T., Zhang, T., Xie, J., et al. (2024). Effects of feeding patterns on production performance, lipo-nutritional quality and gut microbiota of Sunit sheep. *Meat Sci.* 218:109642. doi: 10.1016/j.meatsci.2024.109642
- Keiran, N., Ceperuelo-Mallafré, V., Calvo, E., Hernández-Alvarez, M. I., Ejarque, M., Núñez-Roa, C., et al. (2019). *SUCNR1* controls an anti-inflammatory program in macrophages to regulate the metabolic response to obesity. *Nat. Immunol.* 20, 581–592. doi: 10.1038/s41590-019-0372-7
- Kim, G., Yoon, Y., Park, J. H., Park, J. W., Noh, M. G., Kim, H., et al. (2022). *Bifidobacterial* carbohydrate/nucleoside metabolism enhances oxidative phosphorylation in white adipose tissue to protect against diet-induced obesity. *Microbiome*. 10:188. doi: 10.1186/s40168-022-01374-0
- Lackey, D. E., Lynch, C. J., Olson, K. C., Mostaedi, R., Ali, M., Smith, W. H., et al. (2013). Regulation of adipose branched-chain amino acid catabolism enzyme expression and cross-adipose amino acid flux in human obesity. *Am. J. Physiol. Endocrinol. Metab.* 304, E1175–E1187. doi: 10.1152/ajpendo.00630.2012
- Lairson, L. L., Henrissat, B., Davies, G. J., and Withers, S. G. (2008). Glycosyltransferases: structures, functions, and mechanisms. *Annu. Rev. Biochem.* 77, 521–555. doi: 10.1146/annurev.biochem.76.061005.092322
- Li, B., Hou, P. X., Huang, X. Y., Yuan, Q. H., Xu, W. W., et al. (2025). Changes in quality and aroma compounds of Hu sheep with different backfat thicknesses. *Appl. Food Res.* 5, 2772–5022. doi: 10.1016/j.afres.2025.100777
- Li, M., Wang, S., Li, Y., Zhao, M., Kuang, J., Liang, D., et al. (2022). Gut microbiotabile acid crosstalk contributes to the rebound weight gain after calorie restriction in mice. *Nat. Commun.* 13:2060. doi: 10.1038/s41467-022-29589-7
- Li, R., He, Z., Yan, W., Yu, H., Yi, X., Sha, Y., et al. (2023). Tricaprylin, a medium-chain triglyceride, aggravates high-fat diet-induced fat deposition but improves intestinal health. *Food Funct.* 14, 8797–8813. doi: 10.1039/D3FO01749D
- Liang, C., Qiao, L., Han, Y., Liu, J., Zhang, J., and Liu, W. (2020). Regulatory roles of SREBF1 and SREBF2 in lipid metabolism and deposition in two Chinese representative fat-tailed sheep breeds. *Animals* 10:1317. doi: 10.3390/ani10081317
- Lin, K., Zhu, L., and Yang, L. (2022). Gut and obesity/metabolic disease: focus on microbiota metabolites. *MedComm.* 3:e171. doi: 10.1002/mco2.171
- Liu, S., Yang, Y., Luo, H., Pang, W., and Martin G. B. (2024). Fat deposition and partitioning for meat production in cattle and sheep. *Anim. Nutr.* 17, 376–386. doi: 10.1016/j.aninu.2024.03.003
- Lu, D., Wang, W., Li, X., Wang, L., Guo, Y., Zhu, C., et al. (2024). Identification and characterization of a PL35 GAGs lyase with 4-O-sulfated N-acetylgalactosamine (A-type)-rich structures producing property. *Int. J. Biol. Macromol.* 266:131283. doi:10.1016/j.ijbiomac.2024.131283
- Mihas, A. A., Gibson, R. G., Mihas, T. A., and Hirschowitz, B. I. (1981). Sensitivity of serum glutamic oxaloacetic transaminase and bile acid levels for the detection of experimental liver injury in rats. *J. Med.* 12, 237–242.
- Moszak, M., Szulińska, M., and Bogdański, P. (2020). You are what you eat-the relationship between diet, microbiota, and metabolic disorders-a review. *Nutrients*. 12:1096. doi: 10.3390/nu12041096

- Nakamura, A. M., Nascimento, A. S., and Polikarpov, I. (2017). Structural diversity of carbohydrate esterases. *Biotechnol. Res. Innov.* 1, 35–51. doi: 10.1016/j.biori.2017.02.001
- Omer, E., and Chiodi, C. (2024). Fat digestion and absorption: normal physiology and pathophysiology of malabsorption, including diagnostic testing. *Nutr. Clin. Pract.* 39, S6-S16. doi: 10.1002/ncp.11130
- Prentki, M., and Madiraju, S. R. (2008). Glycerolipid metabolism and signaling in health and disease. *Endocr. Rev.* 29, 647–676. doi: 10.1210/er.2008-0007
- Qiu, Y., Wu, L., Zhou, W., Wang, F., Li, N., Wang, H., et al. (2024). Day and night reversed feeding aggravates high-fat diet-induced abnormalities in intestinal flora and lipid metabolism in adipose tissue of mice. *J. Nutr.* 154, 2772–2783. doi: 10.1016/j.tinut.2024.06.004
- Rosen, E. D., and Spiegelman, M. (2014). What we talk about when we talk about fat. Cell. 156, 20–44. doi: 10.1016/j.cell.2013.12.012
- Sacks, F. M., Lichtenstein, A. H., Wu, J. H. Y., Appel, L. J., Creager, M. A., Kris-Etherton, P. M., et al. (2017). Dietary fats and cardiovascular disease: a presidential advisory from the american heart association. *Circulation* 136, e1–e23. doi: 10.1161/CIR.0000000000000510
- Sakamoto, M., and Benno, Y. (2006). Reclassification of bacteroides distasonis, Bacteroides goldsteinii and Bacteroides merdae as Parabacteroides distasonis gen. nov., comb. nov., Parabacteroides goldsteinii comb. nov. and Parabacteroides merdae comb. nov. Int. J. Syst. Evol. Microbiol. 56, 1599–1605. doi: 10.1099/ijs.0. 64192-0
- Schlesinger, S., Schwingshackl, L., and Neuenschwander, M. (2019). Dietary fat and risk of type 2 diabetes. *Curr. Opin. Lipidol.* 30, 37–43. doi: 10.1097/MOL.000000000000000567
- Shao, Y., Huo, D., Peng, Q., Pan, Y., Jiang, S., Liu, B., et al. (2017). *Lactobacillus plantarum HNU082-derived* improvements in the intestinal microbiome prevent the development of hyperlipidaemia. *Food. Funct.* 8, 4508–4516. doi: 10.1039/C7FO 00902I
- Wang, K., Liao, M., Zhou, N., Bao, L., Ma, K., Zheng, Z., et al. (2019). *Parabacteroides distasonis* (Alleviates obesity and metabolic dysfunctions via production of succinate and secondary bile acids). *Cell Rep.* 26, 222–235.e5. doi: 10.1016/j.celrep.2018.12.028
- Wang, Y., Wang, M., Chen, J., Li, Y., Kuang, Z., and Dende, C., et al. (2023). The gut microbiota reprograms intestinal lipid metabolism through long noncoding RNA Snhg9. *Science* 381, 851–857. doi: 10.1126/science.ade0522
- Xie, J., Zhu, Y., Pang, C., Gao, L., Yu, H., Lv, W., et al. (2022). Liver function parameters aspartate aminotransferase and total protein predict functional outcome in stroke patients with non-cardioembolism. *Front. Nutr.* 9:918553. doi: 10.3389/fnut.2022.918553
- Yang, Q., Vijayakumar, A., and Kahn, B. B. (2018). Metabolites as regulators of insulin sensitivity and metabolism. *Nat. Rev. Mol. Cell Biol.* 19, 654–672. doi: 10.1038/s41580-018-0044-8
- Yang, Z., Chen, X., Yu, M., Jing, R., Bao, L., Zhao, X., et al. (2024). Metagenomic sequencing identified microbial species in the rumen and cecum microbiome responsible for niacin treatment and related to intramuscular fat content in finishing cattle. *Front. Microbiol.* 15:1334068. doi: 10.3389/fmicb.2024.1334068
- Yu, H., Raza, S. H. A., Pan, Y., Cheng, G., Mei, C., and Zan, L. (2023). Integrative analysis of blood transcriptomics and metabolomics reveals molecular regulation of backfat thickness in qinchuan cattle. *Animals* 13:1060. doi: 10.3390/ani 13061060
- Zhou, L., Raza, S. H. A., Gao, Z., Hou, S., Alwutayd, K. M., Aljohani, A. S. M., et al. (2024). Fat deposition, fatty acid profiles, antioxidant capacity and differentially expressed genes in subcutaneous fat of Tibetan sheep fed wheat-based diets with and without xylanase supplementation. *J. Animal Physiol. Animal Nutr.* 108, 252–263. doi: 10.1111/jpn.13886
- Zhou, Y., Xu, T., Cai, A., Wu, Y., Wei, H., Jiang, S., et al. (2018). Excessive backfat of sows at 109 d of gestation induces lipotoxic placental environment and is associated with declining reproductive performance. *J. Anim. Sci.* 96, 250–257. doi: 10.1093/jas/skx041